Stratospheric eruptions from tropical and extra-tropical volcanoes constrained using high-resolution sulfur isotopes in ice cores

Andrea Burke[1,2], Kathryn A. Moore[1,3], Michael Sigl[4,5], Dan C. Nita[1,6], Joseph R. McConnell[5], and Jess F. Adkins[2]

[1]School of Earth and Environmental Sciences, University of St Andrews, UK
[2]Division of Geological and Planetary Sciences, Caltech, USA
[3]Department of Atmospheric Science, Colorado State University, USA
[4]Climate and Environmental Physics, University of Bern, Switzerland
[5]Division of Hydrologic Sciences, Desert Research Institute, USA
[6] Department of Geology, Babes-Bolyai University, Romania

Abstract

The record of volcanic forcing of climate over the past 2500 years is based primarily on sulfate concentrations in ice cores. Of particular interest are large volcanic eruptions with plumes that reached high altitudes in the stratosphere, as these afford sulfate aerosols the longest residence time in the atmosphere, and thus have the greatest impact on radiative forcing. Sulfur isotopes measured in ice cores can be used to identify these large eruptions because stratospheric sulfur is exposed to UV radiation, which imparts a time-evolving mass independent fractionation (MIF) that is preserved in the ice. However sample size requirements of traditional measurement techniques mean that the MIF signal may be obscured, leading to an inconclusive result. Here we present a new method of measuring sulfur isotopes in ice cores by multi-collector inductively

coupled plasma mass spectrometry, which reduces sample size requirements by three orders of magnitude. Our method allows us to measure samples containing as little as 10 nmol of sulfur, with a precision of 0.11‰ for $\delta^{34}S$ and 0.10‰ for $\Delta^{33}S$, enabling a high-temporal resolution over ice core sulfate peaks. We tested this method on known tropical (Tambora 1815 and Samalas 1257) and extra-tropical (Katmai/Novarupta 1912) stratospheric eruptions from the Tunu2013 ice core in Greenland and the B40 ice core from Antarctica. These high-resolution sulfur isotope records suggest a distinct difference between the signatures of tropical versus extra-tropical eruptions. Furthermore, isotope mass balance on extra-tropical eruptions provides a means to estimate the fraction of sulfate deposited that was derived from the stratosphere. This technique applied to unidentified eruptions in ice cores may thus improve the record of explosive volcanism and its forcing of climate.

Keywords: volcanoes, sulfur, mass-independent fractionation, stratosphere, Katmai, ice cores

1 Introduction

Volcanic eruptions are the main natural external forcing of climate over the past millennium (Schurer, 2013). The SO_2 erupted from volcanoes is oxidized to sulfate in the atmosphere, and these sulfate aerosols reflect incoming radiation, and cool the planet. The largest climatic impacts occur when volcanic eruption columns reach high altitudes in the stratosphere, as the aerosols remain in the atmosphere for longer, with a residence time of a couple of years (Robock,

2000). In contrast, sulfate aerosols that are erupted into the troposphere are efficiently removed on the order of weeks. Accurate reconstruction of climate forcing by large volcanic eruptions is fundamental for deconvolving forced from internal climate variability and for better understanding climate sensitivity to greenhouse gases.

Current state-of-the art volcanic forcing records are based on sulfate concentrations in ice cores, which show peaks above background levels due to volcanic eruptions (e.g. Gao et al., 2007; Sigl et al., 2015). Sulfate concentrations from several cores are spatially averaged to determine the total mass deposition rate (i.e. "flux") of sulfate to the ice sheet for a given eruption, and this is then scaled to a total stratospheric burden of sulfate, which can be used to calculate radiative forcing changes or aerosol optical depth fields (e.g. Toohey and Sigl, 2017). However, sulfate concentrations in ice can also be elevated due to local, smaller eruptions that did not make it to high altitudes in the stratosphere and thus would not have had a large climatic impact. To address this complication, ice core sulfate records from Greenland and Antarctica have been synchronized and compared to determine which sulfate peaks occur in both hemispheres. These peaks are called 'bipolar events', and are attributed to large, tropical eruptions whose plumes made it to the stratosphere and thus were distributed globally, allowing for deposition of sulfate aerosols in both hemispheres (e.g. Plummer et al., 2012; Sigl et al., 2013). These events are then scaled to have a larger effect on the radiative forcing of climate compared to sulfate events that occur in only one of hemispheres (Gao et al., 2008; Sigl et al., 2015; Toohey and Sigl, 2017). However, this approach is not without its difficulties: the attribution of a bipolar event relies on very precise ice core age models, and typical age

uncertainties over the past two thousand years can be of the order of 2-4 years (McConnell et al., 2018; Sigl et al., 2015). Thus, based on sulfate concentration alone it is not possible to distinguish between a bipolar event, and two hemispheric events that occur within age model uncertainty of each other. For mid-to-high latitude eruptions (producing unipolar sulfate signals), it is also not possible to determine how much of the sulfate deposited on the ice sheet came via the stratosphere since a large proportion could be transported tropospherically. Given the large difference in the radiative forcing following eruptions with high stratospheric injection height (i.e. 24 km or higher) compared to eruptions with lower injection heights (Toohey et al., 2019), there is a need for a means to independently constrain volcanic sulfate injections to the high stratosphere.

Sulfur isotopes have been used in polar snow (Baroni et al., 2007) and ice cores (e.g. Baroni et al., 2008; Cole-Dai et al., 2009; Gautier et al., 2019; Savarino, 2003) to distinguish between eruptions whose plumes reached the stratosphere at or above the ozone layer and those that remained below. This approach is possible because the sulfur that makes it up to the ozone layer is exposed to UV radiation, which imparts a mass independent fractionation (MIF) of the S isotopes (Farquhar et al., 2001). This fractionation is then recorded in the ice cores as a non-zero $\Delta^{33}S$ value, where

$$\Delta^{33}S\ (‰) = \delta^{33}S - ((\delta^{34}S + 1)^{0.515} - 1) \quad \text{(Equation 1)}$$

and $\delta^{3x}S = ({}^{x}S/{}^{32}S)_{sample}/({}^{x}S/{}^{32}S)_{reference} - 1$, with x either 33 or 34. Almost all physical, chemical and biological processes fractionate isotopes based on mass, and thus have $\Delta^{33}S$ values that are zero. Sulfur photochemistry is one of the few processes that produces mass-independent fractionation, even though the exact

101 photochemical mechanism for this fractionation is still debated (e.g. Gautier et
102 al., 2018). The presence of non-zero $\Delta^{33}S$ in sulfate in ice therefore indicates that
103 the sulfate formation occurred at a height in the stratosphere where it is possible
104 to interact with UV radiation. Although sulfur isotopes have previously been
105 used as a means to distinguish between stratospheric and tropospheric
106 eruptions (e.g. Lanciki et al., 2012), an important caveat is that at high latitudes,
107 the lower stratosphere lies below the ozone layer (Fig. 1), and so it is possible to
108 have a high latitude eruption that reaches the lower stratosphere that does not
109 result in a MIF signature in polar ice (Schmidt et al., 2012). However, recent
110 modelling work (Toohey et al., 2019) shows that high latitude eruptions that
111 only penetrate into the upper troposphere/lower stratosphere (UT/LS) have
112 reduced radiative forcings because of shorter sulfate aerosol residence times.
113 The unambiguous identification of volcanic events that had plumes that reached
114 altitudes in the stratosphere at or above the ozone layer, and thus had long
115 atmospheric residence times, would represent a major improvement of the
116 record of volcanic forcing of climate.
117 Sulfur isotopes are traditionally measured by gas-source mass
118 spectrometry. These methods require a micromole of sulfur for analysis and
119 thus entire sulfate peaks were analyzed from a single ice core (Baroni et al.,
120 2008) or multiple ice cores were synchronized and combined (Gautier et al.,
121 2019; 2018) to get enough sulfate from an individual eruption . Since the $\Delta^{33}S$
122 signature is time-evolving from positive to negative over the course of the sulfate
123 deposition on the ice sheet (Baroni et al., 2007), the integration over an entire
124 peak may give $\Delta^{33}S = 0$ (Baroni et al., 2008), resulting in ambiguity in the
125 fingerprinting of stratospheric eruptions. To resolve this issue we applied a new

technique of S isotope measurement by MC-ICP-MS to ice cores (McConnell et al., 2017; Paris et al., 2013). This method requires only 10 nmol of sulfate, allowing up to bi-monthly resolution. We applied this technique to two known tropical stratospheric eruptions (Tambora 1815 and Samalas 1257), as well as a known high latitude stratospheric eruption (Katmai/Novarupta 1912) to test the applicability of this approach for volcanic eruptions proximal to the ice sheet.

2 Methods

Ice core samples were collected from the Tunu2013 core from Greenland (78° 2.1' N 33° 52.8' W, 2105 m; 213 m deep; collected May 2013 (Sigl et al., 2015)) for three large volcanic eruptions: the 1815 eruption of Tambora (Indonesia), the 1257 eruption of Samalas (Indonesia), and the 1912 eruption of Katmai/Novarupta, henceforth Katmai (Alaska, US). The eruption of Samalas was also replicated from the B40 core from Antarctica (75° 0' S 0° 4.1' E, 2890 m; 200 m deep; collected December 2012 (Sigl et al., 2014)). The age models and continuous sulfur concentration measurements from these ice cores (Sigl et al., 2015) were used to identify the volcanic peaks. Samples were cut from the wings of cores at a resolution of ~2-3 cm over the course of each volcanic event and a resolution of 5 cm for background analyses pre- and post-event. Each sample was measured twice, so a total of 20 nmol was used (only 4 mL for event samples (5 uM) to 40 mL for background samples (0.5 uM)), making this method preferable for high-resolution work on precious sample material. Outside edges of the ice core were scraped clean and the samples were melted. Sulfate concentration was determined by ion chromatography on a 500 μL aliquot.

These concentrations (circles, Fig 2 a,b, Fig 3 a) were compared to continuous sulfur measurements (Sigl et al., 2015) to validate which part of the peak was sampled in the discrete samples, and to determine the amount of sample needed for two isotope measurements (20 nmol total). The appropriate amount of sample was then dried down and redissolved in 70 μL of 0.01% v/v distilled HCl under clean laboratory conditions. The samples were passed through Teflon columns made from 4:1 PTFE heat shrink tubing (11 mm expanded diameter) that were loaded with 35 μl of clean AG1X8 anion-exchange resin in order to separate out the sulfate from the sample matrix. Prior to sample loading, the resin was cleaned with 350 μl of 1.6 M HNO_3, 350 μl of 1.2 M HCl, and 350 μl of 0.6 M HCl. Samples were then loaded and cations were removed by rinsing the column with 3 times 175 μl of MilliQ water, followed by sulfate elution in 3×70 μl of 0.5 M HNO_3. The eluted samples were evaporated to dryness, resuspended in 0.5 M HNO_3, and NaOH was added to the sample to match the concentration and matrix of the in-house Na_2SO_4 bracketing standard (Paris et al., 2013).

Triple sulfur isotopes (^{32}S, ^{33}S, ^{34}S)[1] were measured by MC-ICP-MS using sample-standard bracketing with an in-house Na_2SO_4 standard (Paris et al., 2013) at both Caltech and the STAiG lab at the University of St Andrews, and are reported relative to Vienna-Canyon Diablo Troilite (V-CDT). Each sample was measured at least twice. Long-term external reproducibility on the Caltech Switzer Falls secondary river water standard (Burke et al., 2018) was $\delta^{34}S$ = 4.11±0.24 and $\Delta^{33}S$ = 0.05 ± 0.18 ‰ (2 s.d., n = 10) at Caltech and $\delta^{34}S$ = 4.17 ±

[1] Although ^{36}S provides further information about the oxidation process in the atmosphere (Gautier et al., 2018), it is not possible to measure ^{36}S by MC-ICP-MS because the argon plasma results in an interference from ^{36}Ar.

0.11 and $\Delta^{33}S$ = 0.01 ± 0.10 ‰ (2 s.d., n = 16) at St Andrews (Supplemental Data Table 3). Procedural blanks were run with each set of columns at Caltech and St Andrews, and the values were 0.12 ± 0.02 nmol with a $\delta^{34}S$ value of -0.2±2.8 ‰ (2 s.d., n = 3) for Caltech and 0.14 ± 0.04 nmol with a $\delta^{34}S$ value of 5.5±1.9 ‰ (2 s.d., n = 9) for St Andrews (Supplemental Data Table 4). All reported $\delta^{34}S$ and $\delta^{33}S$ values were blank corrected with the long-term blank averages, and errors were propagated. $\Delta^{33}S$ values were calculated following Equation 1.

Background ice core samples were measured prior to the volcanic sulfate events. These background samples were used to correct the measured sulfate isotope values (δ_{meas}) for background sulfate to determine the isotope values of the volcanic sulfate (δ_{volc}) following equation 2 (Baroni et al., 2007) :

$$\delta_{volc} = \left(\delta_{meas} - f_{bkgd}\delta_{bkgd}\right)/f_{volc} \quad \text{(Equation 2)}$$

where δ_{bkgd} is the $\delta^{34}S$ or $\delta^{33}S$ of the background sample, f_{bkgd} is the mass fraction of the total sulfate that can be attributed to the background ($f_{bkgd} = [SO_4]_{bkgd}/[SO_4]_{sample}$), and f_{volc} is the mass fraction of the total sulfate that can be attributed to volcanic sulfate ($f_{volc} = 1 - f_{bkgd}$). Following Gautier et al. (2018) we only plotted those samples with more than 65% volcanic sulfate (f_{volc} > 0.65).

3 Results

Each of the three volcanic events show non-zero $\Delta^{33}S$ (Figs 2 and 3, Supplementary Data Table 1), with an evolution from positive to negative over the course of the sulfate deposition (Baroni et al., 2007), and there is good

197 agreement (Fig 4) between the records of the Samalas eruption in Greenland
198 (Tunu2013) and Antarctica (B40). In the Tunu2013 core, the magnitude of the
199 $\Delta^{33}S$ is larger for sulfate associated with the Samalas and Tambora eruptions
200 (1.9‰ and 1.7‰, respectively; Fig 2) than it is for the Katmai eruption, which
201 only has a magnitude of 0.4‰ (Fig 3). The lowest $\Delta^{33}S$ values for the Samalas
202 and Tambora eruptions are negative (-1.8 and -0.8 ‰), whereas the lowest $\Delta^{33}S$
203 values for the Katmai eruptions are within uncertainty of 0‰. In B40, the $\Delta^{33}S$
204 values for Samalas range from 1.4 to -1.5‰.
205 In the two tropical eruptions (Fig 2), $\delta^{34}S$ follows the same shape as the
206 $\Delta^{33}S$, with an initial increase to 27.5‰ for Samalas and 20.6‰ for Tambora,
207 dropping to -19.1‰ and -5.9‰ respectively over the course of the deposition of
208 the sulfate. In contrast, for the Katmai eruption the $\delta^{34}S$ initially decreases from
209 its background value of 7.2‰ down to 0.6‰, before increasing back up to 4.6‰
210 (Fig 3). In B40, the $\delta^{34}S$ values for Samalas range from 17.3 to -12.5‰
211 (Supplementary Data Table 1).
212 Pre-event background samples were measured for both the Samalas and
213 Katmai eruptions. $\delta^{34}S$ values prior to the Samalas event in Tunu2013 ranged
214 from 9.1 to 11.1 ‰ with an average concentration of 0.4 μM, and prior to the
215 Katmai event were 7.2 ‰ at a concentration of 1.3 μM. The $\delta^{34}S$ value prior to
216 the Samalas event in B40 was 13.9‰ at a concentration of 0.6 μM. All
217 background samples had $\Delta^{33}S$ values within uncertainty of 0‰. Although we
218 attempted to measure a pre-event background for Tambora, the sample that was
219 cut from the ice core included the onset of the volcanic sulfate peak, and had a
220 $\Delta^{33}S$ value of 0.5‰. Thus, the average of 13 non-volcanic pre-industrial

background samples from other intervals of the Tunu2013 ice core ($\delta^{34}S$ = 9.2 ± 0.93‰, $\Delta^{33}S$ = 0.03 ± 0.09, [S] = 0.5 ± 0.2 μM; Supplementary Data Table 2) was used to make a background correction for the Tambora samples. This average excludes the background sample for Katmai deposited in 1912, which likely has significant anthropogenic sulfate, supported by its higher concentration and lower isotopic value. The standard deviation of these background samples was used to calculate the final uncertainty on the background-corrected volcanic sulfate $\delta^{34}S$ and $\Delta^{33}S$ values by Monte Carlo simulations.

The background-corrected volcanic sulfate $\Delta^{33}S$ values for the Samalas and Tambora eruptions have a similar positive to negative temporal evolution as the non-background corrected values, but with a larger range (Fig 2). In Tunu2013, the volcanic sulfate $\Delta^{33}S$ values for Samalas and Tambora range from 2.8 to -2.5‰ and from 2.2 to -0.85‰, respectively. The volcanic sulfate $\delta^{34}S$ values for Samalas and Tambora range from 29.7 to -31.1‰ and 23.4 to -7.9‰, respectively. In contrast, the background-corrected volcanic sulfate for the Katmai eruption in Tunu2013 has $\delta^{34}S$ values between 4.4 and -4.3‰ and $\Delta^{33}S$ values between 0.3 and 0.6‰, with a different temporal trend (Fig 3). In B40, the Antarctic core, the volcanic sulfate $\Delta^{33}S$ and $\delta^{34}S$ values for Samalas is very similar to that found in Greenland in Tunu2013, with a range from 1.7 to -2.2‰ and from 19.2 to -24.2‰, respectively (Supplementary Data Table 1).

4 Discussion

4.1 $\Delta^{33}S$ constraints on eruptive plume height

The presence of non-zero $\Delta^{33}S$ in each of these eruptions implies that some of the SO_2 from the eruptive plume reached a height in the stratosphere at least as high as the ozone layer (Fig 1). At these altitudes in the atmosphere the SO_2 was exposed to UV radiation imparting a MIF signal, and this signal was preserved in the sulfate deposited on the ice sheet. For the two tropical eruptions (Tambora and Samalas), this puts a rough constraint of > 20km for the eruptive plume. This height constraint is consistent with estimates of the Tambora and Samalas column height of up to 43 km (Sigurdsson and Carey, 1989; Vidal et al., 2016), which would mean that the SO_2 was transported well above the ozone layer.

For the extra-tropical Katmai eruption (58° N), the presence of non-zero $\Delta^{33}S$ puts a height constraint of >15 km for the eruptive plume, consistent with estimates of a column height of 17-26 km for this eruption (Fierstein and Hildreth, 1992). Previous studies (e.g. Schmidt et al., 2012) have questioned whether MIF signals from high latitude eruptions (i.e. proximal to ice sheets) could be preserved in ice, given that a substantial amount of sulfate would be transported directly to the ice sheet via the troposphere or lower stratosphere below the ozone layer with $\Delta^{33}S = 0‰$. It was hypothesized that this upper tropospheric/lower stratospheric (UT/LS) transport may overwhelm the signal of any MIF from sulfate from at or above the ozone layer. However, our results suggest that the MIF signature can be preserved in ice for high latitude eruptions, albeit more muted (maximum $\Delta^{33}S$ values of ~0.5‰) than in tropical eruptions (maximum $\Delta^{33}S$ values of ~2‰) where none of the sulfate was delivered to the ice sheets directly via the troposphere. Thus, the presence of non-zero $\Delta^{33}S$ in volcanic sulfate in ice cores provides a minimum height of the eruptive plume

into the stratosphere above the ozone layer, even if the volcano was from the high latitudes. This minimum height will be useful in characterizing the climatic forcing of unknown eruptions because volcanic aerosols that make it to higher altitudes in the stratosphere have a longer residence time, and thus a greater negative radiative forcing, than aerosols that remain in the troposphere (or in the lower levels of the stratosphere below the ozone layer) (Toohey et al., 2019).

4.2 Time evolving signature of $\Delta^{33}S$ and $\delta^{34}S$ and fingerprinting of tropical and extratropical eruptions

For all three eruptions, the $\Delta^{33}S$ follows a time evolving signature where the initial sulfate deposited has a positive $\Delta^{33}S$, and the later sulfate has a negative $\Delta^{33}S$ (Fig 2). This time evolution has been observed before (Baroni et al., 2007) from measurements of sulfate from the 1991 eruption of Pinatubo (Philippines) and the 1963 eruption of Agung (Indonesia) collected from snow pits in Antarctica, and more recently from combined multiple ice cores (Gautier et al., 2018). The initial fractionation process generates a positive $\Delta^{33}S$, and the following negative $\Delta^{33}S$ is a result of mass balance (Baroni et al., 2007), with the $\Delta^{33}S$ excursion evolving over a timescale of about 3 to 4 years (Fig 2). Given that the timescale over which sulfur dioxide is oxidized to sulfate in the atmosphere is approximately a month, in order to generate the observed isotopic signature that is deposited in the ice over the course of several years there needs to be a spatial separation of these sulfur pools with a differing $\Delta^{33}S$ signature (Gautier et al., 2018).

293 We can use the timing and the shape of the $\Delta^{33}S$ and $\delta^{34}S$ signatures to
294 fingerprint whether the sulfate from a volcanic event in an ice core was purely
295 stratospheric (and thus likely tropical) or if some of the sulfate was transported
296 to the ice sheet via the troposphere (or lower stratosphere below the ozone
297 layer), and thus likely came from an extra-tropical eruption in the hemisphere of
298 the ice sheet. In the case of the two tropical eruptions (Fig 2), the peak in the
299 $\Delta^{33}S$ comes at the very start of the sulfate deposition; this was also observed in
300 the case of the Pinatubo and Agung eruptions (Baroni et al., 2007). In contrast,
301 for the Katmai eruption (Fig 3), the initial sulfate deposited to the ice sheet has a
302 $\Delta^{33}S = 0‰$ because in the case of this high latitude eruption the first sulfate to
303 arrive to the ice sheet was transported via the troposphere (or lower
304 stratosphere below the ozone layer) and thus was not fractionated.
305 The $\delta^{34}S$ of the tropical eruptions show a strong positive correlation
306 between the $\Delta^{33}S$ and the $\delta^{34}S$ ($r^2 > 0.99$; Fig 5); the initial sulfate $\delta^{34}S$ increases
307 and then decreases over the same timeframe as the $\Delta^{33}S$ changes. The strong
308 correlation is because the same process that causes the non-zero $\Delta^{33}S$
309 fractionation in the stratosphere also drives fractionation observed in $\delta^{34}S$, and
310 since the sulfate in these peaks from tropical eruptions is derived purely from
311 the stratosphere, this signature is preserved. In contrast, for the Katmai eruption,
312 the initial volcanic sulfate decreases the $\delta^{34}S$ values compared to background
313 $\delta^{34}S$ values. This feature can be understood by mass balance: background sulfate
314 is around 10‰ as it is a mixture of marine (21‰) and volcanic emissions
315 (~0‰), and thus the addition of more volcanic sulfate with low $\delta^{34}S$ (that has
316 not been fractionated by stratospheric processes as in the case of the tropical

317 eruptions) would act to decrease the $\delta^{34}S$. This is the opposite of what is
318 measured in the initial $\delta^{34}S$ in the tropical eruptions and thus can provide an
319 additional means of distinguishing between unknown tropical and extra-tropical
320 events recorded in ice cores. In contrast to the tropical eruptions, the correlation
321 between $\delta^{34}S$ and $\Delta^{33}S$ in the sulfate from the Katmai eruption is weak ($r^2 = 0.37$)
322 and negative (slope is -0.05).
323 Distinguishing between tropical and extra-tropical eruptions in the ice
324 core record of volcanism is important for improving the volcanic radiative
325 forcing record for two reasons. Firstly, constraining the latitudinal band of
326 eruptions has implications for transport and residence time of climatically
327 important aerosols. Secondly, if a fraction of the sulfate deposited in the ice core
328 was delivered through the troposphere, then the associated radiative forcing for
329 that event should be adjusted, as current reconstructions assume that all sulfate
330 deposited in the ice reached the stratosphere (e.g. Toohey and Sigl, 2017). High-
331 resolution sulfur isotope measurements in ice cores thus can potentially provide
332 an additional means of distinguishing between unknown tropical and extra-
333 tropical events recorded in ice cores if this observation is corroborated by
334 further studies.
335
336 **4.3 Agreement of isotope records between hemispheres**
337 There is good agreement between the two $\Delta^{33}S$ records from Greenland
338 (Tunu2013) and Antarctica (B40) for the Samalas eruption (Fig 4). This
339 agreement suggests that the isotopic signature is primary and is not significantly
340 affected or altered by transport or depositional processes. Furthermore, all
341 three records of tropical eruptions (Tambora from Tunu2013, and Samalas from

342 Tunu2013 and B40) plot along the same line in $\Delta^{33}S$ versus $\delta^{34}S$ space within
343 uncertainty (Fig 5; Table 1). The slope of this line is 0.089 ± 0.003 and is the
344 same as the slope of the line derived from eight eruptions from Antarctic ice
345 (0.09±0.02) (Gautier et al., 2018), but is more precisely constrained. When
346 plotted in $\ln(\delta^{33}S +1)$ versus $\ln(\delta^{34}S +1)$ space, the slope of the line is 0.608 ±
347 0.006, significantly different from the terrestrial mass dependent slope of 0.515.
348 Thus, the relationship between $\delta^{33}S$ and $\delta^{34}S$ for volcanic sulfate derived from
349 the stratosphere is predictable and does not appear to differ between ice cores
350 or eruptions. Differences in aerosol transport or deposition, or indeed the
351 timing, hemisphere, or magnitude of the eruption, therefore do not appear to
352 significantly affect the fractionation process (Gautier et al., 2018). This
353 predictable relationship between $\delta^{33}S$ and $\delta^{34}S$ for volcanic sulfate derived from
354 the stratosphere proves useful in estimating the proportion of stratospheric
355 sulfate from extra-tropical eruptions (see section 4.4).
356 It remains an open question as to what exact process causes this sulfur
357 isotope fractionation. Gautier et al.(2018) use both $\Delta^{33}S$ and $\Delta^{36}S$ data from ice
358 cores to estimate the proportion of different oxidation pathways that could
359 explain the isotopic trends. While their data cannot rule out or unambiguously
360 confirm an oxidation pathway, they show that mass independent oxidation
361 pathways (e.g. photolysis or photoexcitation) could account for at least 21% and
362 as much as 91% of the oxidation. Furthermore, they argue that the small
363 variations in the slope in $\Delta^{33}S$ versus $\delta^{34}S$ space (further confirmed in this study)
364 imply that the relative contribution of different oxidation pathways is similar
365 across eruptions. If the oxidation pathways are similar across different
366 eruptions, then the differences in the magnitude of the mass independent

fractionation between eruptions need to be explained by another process. A recent study (Lin et al., 2018) that considered the correlation between cosmogenic ^{35}S and $\Delta^{33}S$ in modern aerosols proposed that the $\Delta^{33}S$ signature is altitude dependent, with greater fractionation occurring higher in the stratosphere. If true, this would prove a useful metric for estimating eruptive plume height in past eruptions, and improving the record of the volcanic forcing of climate.

4.4 Proportion of stratospheric sulfate from Katmai

We can use the high-resolution isotope record from the Katmai eruption and isotope mass balance to calculate the proportion of sulfate that was deposited in the Greenland ice core via the stratosphere. This calculation will improve volcanic forcing indices since these indices typically make the assumption that all of the sulfate deposited on the ice sheets was stratospheric (Toohey and Sigl, 2017), which is likely incorrect in the case of high latitude eruptions such as Katmai. This calculation is based on the following two isotope mass balance equations:

$$\delta^{34}S_{meas} = \delta^{34}S_{strat} f_{strat} + \delta^{34}S_{trop}\left(1 - f_{strat}\right) \quad \text{(Equation 3)}$$

$$\delta^{33}S_{meas} = \delta^{33}S_{strat} f_{strat} + \delta^{33}S_{trop}\left(1 - f_{strat}\right) \quad \text{(Equation 4)}$$

where the subscript *meas* refers to measured isotopic values, f_{strat} refers to the fraction of sulfate deposited that came from the stratosphere, and the subscripts *strat* and *trop* refer to the isotopic composition of the sulfate coming from the stratosphere and troposphere respectively. Since sulfate formed in the

troposphere (and lower stratosphere below the ozone layer) follows terrestrial mass dependent fractionation, we can use the following relationship:

$$\delta^{33}S_{trop} = \left(\left(\delta^{34}S_{trop} + 1\right)^{0.515} - 1\right) \quad \text{(Equation 5)}$$

to reduce the number of unknowns in those paired equations. We can further reduce the number of unknowns since the stratospheric sulfate measured in ice cores follows the following relationship (see Section 4.3):

$$\delta^{33}S_{strat} = ((\delta^{34}S_{strat} + 1)^{0.608} - 1) \quad \text{(Equation 6)}$$

with an uncertainty on the exponent λ = 0.608 of 0.006. Combining equations 3 to 6 gives two equations with three unknowns: $\delta^{34}S_{strat}$, $\delta^{34}S_{trop}$, and f_{strat}. Thus if we make an assumption of the isotopic composition of the volcanic $\delta^{34}S_{trop}$, we can solve for f_{strat} and $\delta^{34}S_{strat.}$. The sulfur isotopic composition of volcanic SO_2 can vary significantly away from a mantle value (0‰, V-CDT) as a function of the mantle source and the oxygen fugacity of the magma (e.g. de Moor et al., 2010; Mather et al., 2006). To address this, we calculate the f_{strat} and corresponding uncertainty using a 500 iteration Monte Carlo simulation for a uniformly distributed range of $\delta^{34}S_{trop}$ values from -10 to 10‰. The uncertainties on the measured values and exponent λ are assumed to be normally distributed. We find that the f_{strat} values for the Katmai samples range from 0.26 to 0.88, and that when integrated over the whole peak, the proportion of the sulfate peak that came from the stratosphere was 0.55, with an uncertainty range of 0.35 to 0.62. Constraints on the $\delta^{34}S_{trop}$ for this specific eruption would help to narrow the range of uncertainty of the fraction of stratospheric sulfate deposited in Greenland. Even so, this estimate improves upon the assumption that all of the sulfate deposited came from the stratosphere (Toohey and Sigl, 2017). It also

414 helps to reconcile estimates of stratospheric sulfate loading from studies using
415 pyrheliometric optical depth perturbations with estimates based purely on the
416 sulfate deposition in Greenland, which are greater than the optical depth
417 estimates by a factor of three (11 Tg compared to 30 Tg (Hammer et al., 1980;
418 Stothers, 1996)). This approach may thus be used in future studies to improve
419 volcanic forcing indices.
420
421 **5. Conclusion**
422
423 Sulfur isotopes of volcanic sulfate deposited in ice cores can be used to
424 identify if the sulfate came from above the ozone layer in the stratosphere, since
425 exposure to UV radiation imparts a mass independent fractionation, recorded as
426 a non-zero $\Delta^{33}S$ (Savarino et al., 2003). There is good agreement between
427 isotope records from Greenland and Antarctica over the same volcanic event,
428 indicating that sulfur isotopes are not significantly affected by transportation or
429 depositional processes. Our method of analysis by MC-ICPMS requires only 10
430 nmol of sulfur, allowing for up to bi-monthly resolution over the volcanic sulfate
431 peak in the ice cores from samples as small as 4 mL. These high-resolution
432 records show distinct differences between tropical (Samalas and Tambora) and
433 extra-tropical (Katmai) eruptions. In the case of the tropical eruptions, all of the
434 sulfate deposited on the ice sheet came via the stratosphere, and thus the $\delta^{34}S$
435 and $\Delta^{33}S$ values are strongly correlated, with the initial sulfate deposited
436 showing an increase in both values. In contrast, for the extra-tropical eruption,
437 some of the sulfate was deposited in Greenland via the troposphere or lower
438 stratosphere below the ozone layer, and thus the initial signal of the volcanic

sulfate is a decrease in its $\delta^{34}S$ value, with $\Delta^{33}S$ values within error of zero. Isotope mass balance on extra-tropical eruptions such as Katmai can be used to estimate the proportion of the volcanic sulfate deposited in the ice core that came via the stratosphere. These measurements will help to improve the record of the volcanic forcing of climate for unidentified eruptions in the past, which should in turn improve simulations of historical climate change.

Acknowledgements

This research was funded by a Foster and Coco Stanback postdoctoral fellowship and a Marie Curie Career Integration Grant (CIG14-631752) to AB and a NSF-OCE grant 1340174 and NSF-EAR grant 1349858 to JFA. MS acknowledges funding from the European Research Council (ERC) under the European Union's Horizon 2020 research and innovation programme (grant agreement No 820047) NSF-PLR grant 1204176 to JRM supported collection and analysis of the Tunu2013 core. We thank Sepp Kipfstuhl of the Alfred Wegener Institut for providing the B40 core. We thank Joel Savarino, an anonymous reviewer, and James Rae for comments on this manuscript.

References

Baroni, M., Savarino, J., Cole-Dai, J., Rai, V.K., Thiemens, M.H., 2008. Anomalous sulfur isotope compositions of volcanic sulfate over the last millennium in Antarctic ice cores. Journal of Geophysical Research 113, D20112. doi:10.1029/2008JD010185

Baroni, M., Thiemens, M.H., Delmas, R.J., Savarino, J., 2007. Mass-Independent Sulfur Isotopic Compositions in Stratospheric Volcanic Eruptions. Science 315, 84–87. doi:10.1126/science.1131754

Burke, A., Present, T.M., Paris, G., Rae, E.C.M., Sandilands, B.H., Gaillardet, J., Peucker-Ehrenbrink, B., Fischer, W.W., McClelland, J.W., Spencer, R.G.M., Voss, B.M., Adkins, J.F., 2018. Sulfur isotopes in rivers: Insights into global weathering budgets, pyrite oxidation, and the modern sulfur cycle. Earth and Planetary Science Letters 496, 168–177. doi:10.1016/j.epsl.2018.05.022

Cole-Dai, J., Ferris, D., Lanciki, A., Savarino, J., Baroni, M., Thiemens, M.H., 2009.

Cold decade (AD 1810–1819) caused by Tambora (1815) and another (1809) stratospheric volcanic eruption. Geophys. Res. Lett. 36. doi:10.1029/2009GL040882

de Moor, J.M., Fischer, T.P., Sharp, Z.D., Hauri, E.H., Hilton, D.R., Atudorei, V., 2010. Sulfur isotope fractionation during the May 2003 eruption of Anatahan volcano, Mariana Islands: Implications for sulfur sources and plume processes. Geochimica et Cosmochimica Acta 74, 5382–5397. doi:10.1016/j.gca.2010.06.027

Farquhar, J., Savarino, J., Airieau, S., and Thiemens, M. H., 2001. Observation of wavelength-sensitive mass-independent sulfur isotope effects during SO2 photolysis: Application to the early atmosphere, J. Geophys. Res., 106, 32829-32840, 10.1029/2000JE001437.

Fierstein, J., Hildreth, W., 1992. The Plinian Eruptions of 1912 at Novarupta, Katmai-National-Park, Alaska. Bull Volcanol 54, 646–684. doi:10.1007/BF00430778

Gao, C., Oman, L., Robock, A., Stenchikov, G.L., 2007. Atmospheric volcanic loading derived from bipolar ice cores: Accounting for the spatial distribution of volcanic deposition. Journal of Geophysical Research 112, D09109. doi:10.1029/2006JD007461

Gao, C., Robock, A., Ammann, C., 2008. Volcanic forcing of climate over the past 1500 years: An improved ice core-based index for climate models. Journal of Geophysical Research 113, D23111. doi:10.1029/2008JD010239

Gautier, E., Savarino, J., Erbland, J., Farquhar, J., 2018. SO 2Oxidation Kinetics Leave a Consistent Isotopic Imprint on Volcanic Ice Core Sulfate. J. Geophys. Res. Atmos. 117, D06216–12. doi:10.1029/2018JD028456

Gautier, E., Savarino, J., Hoek, J., Erbland, J., Caillon, N., Hattori, S., Yoshida, N., Albalat, E., Albarede, F., Farquhar, J., 2019. 2600-years of stratospheric volcanism through sulfate isotopes. Nature Communications 10, 1–7. doi:10.1038/s41467-019-08357-0

Hammer, C.U., Clausen, H.B., Dansgaard, W., 1980. Greenland ice sheet evidence of post-glacial volcanism and its climatic impact. Nature Publishing Group 288, 230–235. doi:10.1038/288230a0

Lanciki, A., Cole-Dai, J., Thiemens, M.H., Savarino, J., 2012. Sulfur isotope evidence of little or no stratospheric impact by the 1783 Laki volcanic eruption. Geophys. Res. Lett. 39, n/a–n/a. doi:10.1029/2011GL050075

Lin, M., Zhang, X., Li, M., Xu, Y., Zhang, Z., Tao, J., Su, B., Liu, L., Shen, Y., Thiemens, M.H., 2018. Five-S-isotope evidence of two distinct mass-independent sulfur isotope effects and implications for the modern and Archean atmospheres. Proceedings of the National Academy of Sciences 115, 8541–8546. doi:10.1073/pnas.1803420115

Mather, T.A., McCabe, J.R., Rai, V.K., Thiemens, M.H., Pyle, D.M., Heaton, T.H.E., Sloane, H.J., Fern, G.R., 2006. Oxygen and sulfur isotopic composition of volcanic sulfate aerosol at the point of emission. Journal of Geophysical Research 111, 1685–9. doi:10.1029/2005JD006584

McConnell, J.R., Burke, A., Dunbar, N.W., Kohler, P., Thomas, J.L., Arienzo, M.M., Chellman, N.J., Maselli, O.J., Sigl, M., Adkins, J.F., Baggenstos, D., Burkhart, J.F., Brook, E.J., Buizert, C., Cole-Dai, J., Fudge, T.J., Knorr, G., Graf, H.-F., Grieman, M.M., Iverson, N., McGwire, K.C., Mulvaney, R., Paris, G., Rhodes, R.H., Saltzman, E.S., Severinghaus, J.P., Steffensen, J.P., Taylor, K.C., Winckler, G.,

519 2017. Synchronous volcanic eruptions and abrupt climate change ~17.7 ka
520 plausibly linked by stratospheric ozone depletion. Proceedings of the
521 National Academy of Sciences 114, 10035–10040.
522 doi:10.1073/pnas.1705595114
523 McConnell, J.R., Wilson, A.I., Stohl, A., Arienzo, M.M., Chellman, N.J., Eckhardt, S.,
524 Thompson, E.M., Pollard, A.M., Steffensen, J.P., 2018. Lead pollution recorded
525 in Greenland ice indicates European emissions tracked plagues, wars, and
526 imperial expansion during antiquity. Proceedings of the National Academy of
527 Sciences 115, 5726–5731. doi:10.1073/pnas.1721818115
528 Paris, G., Sessions, A.L., Subhas, A.V., Adkins, J.F., 2013. MC-ICP-MS measurement
529 of δ 34 S andΔ 33 S in small amounts of dissolved sulfate. Chemical Geology
530 345, 50–61. doi:10.1016/j.chemgeo.2013.02.022
531 Plummer, C.T., Curran, M.A.J., van Ommen, T.D., Rasmussen, S.O., Moy, A.D.,
532 Vance, T.R., Clausen, H.B., Vinther, B.M., Mayewski, P.A., 2012. An
533 independently dated 2000-yr volcanic record from Law Dome, East
534 Antarctica, including a new perspective on the dating of the 1450s CE
535 eruption of Kuwae, Vanuatu. Clim. Past 8, 1929–1940. doi:10.5194/cp-8-
536 1929-2012
537 Robock, A., 2000. Volcanic eruptions and climate. Rev. Geophys. 38, 191–219.
538 doi:10.1029/1998RG000054
539 Savarino, J., 2003. UV induced mass-independent sulfur isotope fractionation in
540 stratospheric volcanic sulfate. Geophys. Res. Lett. 30, 2131.
541 doi:10.1029/2003GL018134
542 Schmidt, A., Thordarson, T., Oman, L.D., Robock, A., Self, S., 2012. Climatic impact
543 of the long-lasting 1783 Laki eruption: Inapplicability of mass-independent
544 sulfur isotopic composition measurements. Journal of Geophysical Research
545 117, n/a–n/a. doi:10.1029/2012JD018414
546 Schurer, A.P., 2013. Small influence of solar variability on climate over the past
547 millennium. Nature Geoscience 7, 1–5. doi:10.1038/ngeo2040
548 Sigl, M., McConnell, J.R., Layman, L., Maselli, O., McGwire, K., Pasteris, D., Dahl-
549 Jensen, D., Steffensen, J.P., Vinther, B., Edwards, R., Mulvaney, R., Kipfstuhl, S.,
550 2013. A new bipolar ice core record of volcanism from WAIS Divide and
551 NEEM and implications for climate forcing of the last 2000 years. J. Geophys.
552 Res. Atmos. 118, 1151–1169. doi:10.1029/2012JD018603
553 Sigl, M., McConnell, J.R., Toohey, M., Curran, M., Das, S.B., Edwards, R., Isaksson, E.,
554 Kawamura, K., Kipfstuhl, S., Krüger, K., Layman, L., Maselli, O.J., Motizuki, Y.,
555 Motoyama, H., Pasteris, D.R., Severi, M., 2014. Insights from Antarctica on
556 volcanic forcing during the Common Era. Nature Clim Change 4, 693–697.
557 doi:10.1038/nclimate2293
558 Sigl, M., Winstrup, M., McConnell, J.R., Welten, K.C., Plunkett, G., Ludlow, F.,
559 Büntgen, U., Caffee, M., Chellman, N., Dahl-Jensen, D., Fischer, H., Kipfstuhl, S.,
560 Kostick, C., Maselli, O.J., Mekhaldi, F., Mulvaney, R., Muscheler, R., Pasteris,
561 D.R., Pilcher, J.R., Salzer, M., Schüpbach, S., Steffensen, J.P., Vinther, B.M.,
562 Woodruff, T.E., 2015. Timing and climate forcing of volcanic eruptions for the
563 past 2,500 years. Nature 523, 543–549. doi:10.1038/nature14565
564 Sigurdsson, H., Carey, S., 1989. Plinian and co-ignimbrite tephra fall from the
565 1815 eruption of Tambora volcano. Bull Volcanol 51, 243–270.
566 doi:10.1007/BF01073515
567 Stothers, R.B., 1996. Major optical depth perturbations to the stratosphere from

volcanic eruptions: Pyrheliometric period, 1881–1960. J. Geophys. Res. Atmos. doi:10.1029/95JD03237/pdf

Toohey, M., ger, K.K.X., Schmidt, H., Timmreck, C., Sigl, M., Stoffel, M., Wilson, R., 2019. Disproportionately strong climate forcing from extratropical explosive volcanic eruptions. Nature Geoscience 12, 1–10. doi:10.1038/s41561-018-0286-2

Toohey, M., Sigl, M., 2017. Volcanic stratospheric sulfur injections and aerosol optical depth from 500 BCE to 1900 CE. earth-syst-sci-data.net 9, 809–831. doi:10.1594/WDCC/eVolv2k_v2

Vidal, C.M., Métrich, N., Komorowski, J.-C., Pratomo, I., Michel, A., Kartadinata, N., Robert, V., Lavigne, F., 2016. The 1257 Samalas eruption (Lombok, Indonesia): the single greatest stratospheric gas release of the Common Era. Sci. Rep. 6, 1–13. doi:10.1038/srep34868

583 **Figures**

584

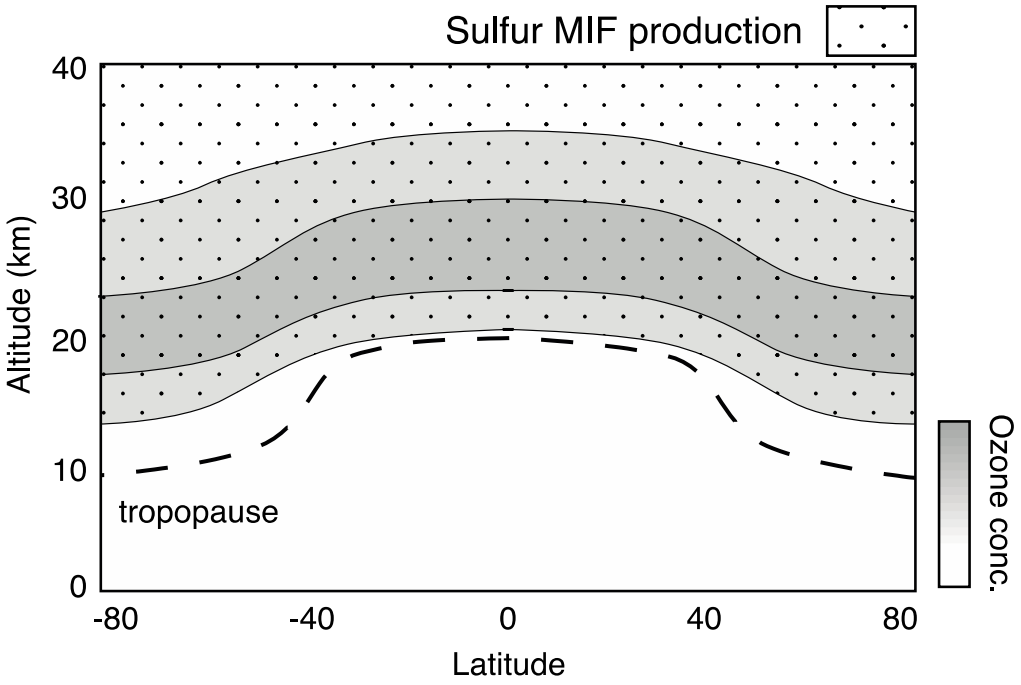

585

586 **Fig 1.** Schematic of sulfur mass independent fractionation (MIF) production. The
587 formation of sulfur MIF requires UV radiation, and therefore it is limited to
588 altitudes in the stratosphere at or above the ozone layer (indicated on schematic
589 by stippling). Without knowing the exact mechanism of sulfur MIF formation it is
590 not currently possible to put more precise altitude constraints on the process. At
591 high latitudes there is a region of the stratosphere that lies below the ozone layer
592 where MIF is not produced. Thus the presence of MIF in polar ice provides a
593 means to identify eruptions whose plumes reached high altitudes in the
594 stratosphere; high latitude eruptions into the lower stratosphere would not
595 produce sulfur MIF.

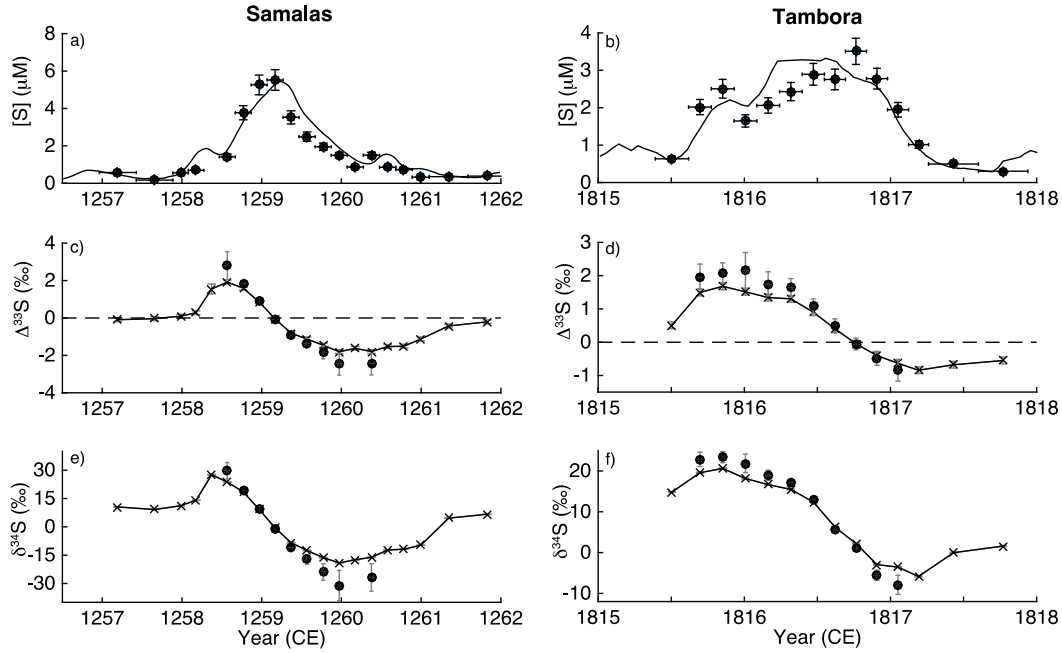

596

597 **Fig 2.** Sulfur concentration (a, b) and isotope curves (c-f) versus time for two
598 tropical eruptions recorded in Tunu2013 ice core in Greenland: the 1258
599 eruption of Samalas (a,c,f) and the 1815 eruption of Tambora (b,d,e). The line in
600 (a,b) is the continuous melting sulfur concentration from (Sigl et al., 2015) and it
601 is compared to sulfur concentration measurements by ion chromatograph on the
602 discrete samples that were subsequently measured for isotopes (circles). (c,d)
603 $\Delta^{33}S$ (‰) measured in the ice samples (x's) and the background corrected
604 volcanic $\Delta^{33}S$ (circles) for samples with more than 65% volcanic sulfate (see
605 text). (e,f) is the same as (c,d), but for $\delta^{34}S$ (‰, V-CDT).

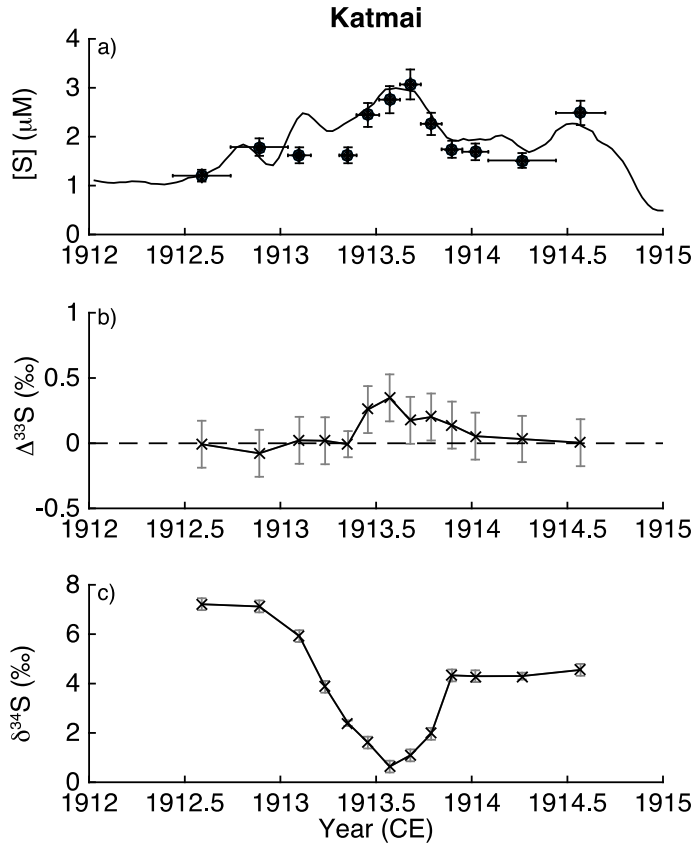

606

607 **Fig 3.** Sulfur concentration (a), $\Delta^{33}S$ (b), and $\delta^{34}S$ (c) versus time for the high

608 latitude eruption Katmai/Novarupta in 1912. The symbols are the same as in

609 Figure 2.

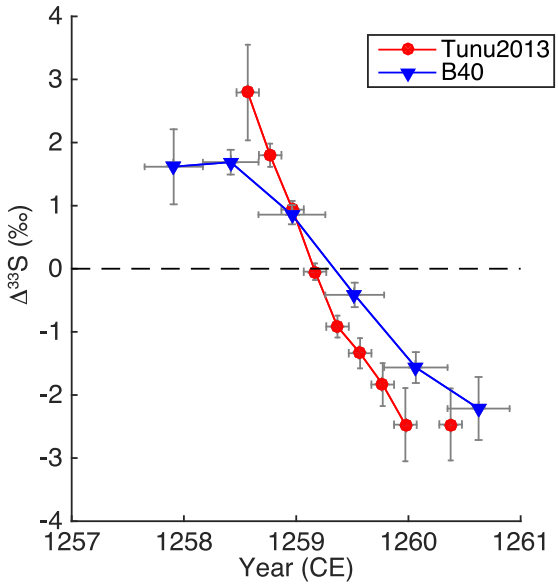

610

611 **Fig 4.** Background-corrected volcanic $\Delta^{33}S$ (‰) across the Samalas volcanic

612 event from the Tunu2013 ice core (Greenland, red circles) and the B40 ice core

613 (Antarctica, blue triangles).

614

615

616

617

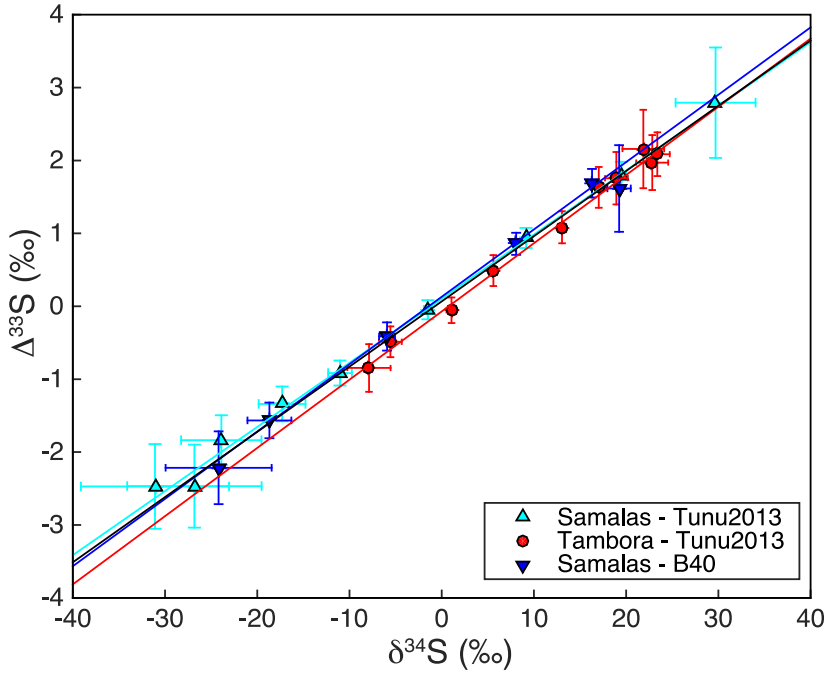

618

619 **Fig 5.** Cross plot of $\Delta^{33}S$ versus $\delta^{34}S$ for the background-corrected volcanic

620 sulfate from tropical eruptions Tambora (red circles) and Samalas (cyan upward

621 triangle measured in Tunu2013, blue downward triangle measured in B40).

622 Regression lines are plotted in the color of the symbols. Black line is the

623 regression considering all of the data. The size of the error bars is driven by

624 uncertainty in the background correction, as analytical uncertainties are ~0.1‰

625 for both $\Delta^{33}S$ and $\delta^{34}S$.

626

627

628

629

630

631

632

633 **Table 1. Regression solution parameters.** Slope and intercept values for linear
634 regressions of $\Delta^{33}S$ versus $\delta^{34}S$ data and $\ln(\delta^{33}S+1)$ versus $\ln(\delta^{34}S+1)$ data for each
635 individual tropical eruption and for all data combined. Uncertainties encompass
636 the 95% confidence interval.

637

638

		$\Delta^{33}S$ versus $\delta^{34}S$		$\ln(\delta^{33}S+1)$ versus $\ln(\delta^{34}S+1)$	
Eruption	**Core**	**slope**	**intercept**	**slope**	**intercept**
Samalas	Tunu2013	0.088±0.003	0.10±0.03	0.604±0.003	0.1±0.05
Samalas	B40	0.092±0.007	0.13±0.04	0.610±0.006	0.1±0.1
Tambora	Tunu2013	0.094±0.005	-0.07±0.08	0.609±0.006	-0.08±0.07
All data		**0.089±0.003**	**0.07±0.05**	**0.608±0.006**	**0.06±0.07**

639

640